PHYSICAL REVIEW A VOLUME 15, NUMBER 2 FEBRUARY 1977

Perturbation approach to the classical one-component plasma*

D. M. Ceperley and G. V. Chester
Laboratory of Atomic and Solid State Physics, Cornell University, Ithaca, New York 14850
(Received 14 May 1976)

The two-particle correlation function for the classical one-component plasma in the high-density fluid phase is calculated from the correlation function of a short-range reference potential by a perturbation method based on the hypernetted chain equation (HNC). It is shown that the long-wavelength correlations are correctly described by this method. A technique for extending $g(r)$ to infinity is shown to be valid and useful. The results are in excellent agreement with those obtained from the "Ewald image" Monte Carlo method.

INTRODUCTION

Many thermodynamic systems in nature have long-range Coulomb forces acting between the constituent particles. The two types of computer simulation, molecular dynamics (MD) and Monte Carlo (MC), have filled an important gap between theory and experiment in the study of such systems. But both of these methods are limited, at the present time, to systems of at most several thousand particles; whereas the actual potential may extend over millions of particles.

The standard method for simulating such a system is to replace the long-range potential with a finite-range "Ewald image potential."[1] The simulation must be performed with periodic boundary conditions; this is the usual way to make a finite system behave like an infinite homogeneous medium. The Ewald image potential is the interaction between one particle and *all* of the images of another particle in the periodically extended space. This effective interaction between two particles is no longer spherically symmetric; for computational purposes it can be approximated by a spherically symmetric part plus a few cubic harmonics. This method has been used to find the equilibrium properties of the classical one-component plasma at densities where other theoretical techniques do not work.[1,2]

There are several reasons for developing and testing an alternative to the Ewald image method. First, the Ewald method is somewhat awkward and time consuming computationally because the evaluation of the potential will take many times longer than a central potential. Second, the image potential is not radially symmetric, as is the actual potential, and this may influence the equilibrium state. In particular, the equilibrium correlation function $g(\vec{r})$ is not radially symmetric even when the potential is, because the boundary is a cube. The addition of the unsymmetric long-range Ewald potential may enhance the cubic symmetry in $g(\vec{r})$, for example, by favoring lattice-like configurations. Recently Valleau and Whittington[3] have pointed out that the Ewald potential allows interactions which are not present in an infinite homogeneous Coulomb system. If there is a fluctuation in the simulation cube, for example, a dipole moment is formed, the fluctuation will be replicated in the image cubes. These fluctuations are allowed to interact with the Ewald potential. In an infinite system the polarization of one section of the system will produce a spatially varying polarization in the surrounding region. Also the periodic boundary conditions allow only density fluctuations with a discrete set of wave vectors; for a plasma the long-range correlations involving small wave vectors are very important. Third, the one-component plasma is a good system to test some of the perturbation techniques that calculate the equilibrium properties of a long-range system in terms of a short-range one. The only complication in the plasma is the presence of the long-range force. On the other hand, the long-range correlations in this system are known exactly.[4]

Briefly, the method we describe and test here consists in calculating the two-particle correlation function for a suitable short-range potential, extending it to infinity, and applying a perturbation method based on the HNC equation to find the equilibrium properties of the one-component plasma. The excellent agreement we find provides an important check on the validity of the standard Ewald method. As far as we know this is the first independent check of this method.

The one-component plasma

The thermodynamic system studied in this paper is the classical one-component plasma (OCP) in the fluid phase at densities near the classical liquid-solid transition. There is a simple Coulomb potential between particles, and the system is immersed in a uniform background of opposite charged particles to make the energy of the system extensive. In this paper the conventional dimen-

sionless units[1] are used throughout (the density $\rho = 3/4\pi$, the inverse temperature is $\beta = 1/kT = 1$). In these units

$$V(r) = \Gamma/r , \tag{1}$$

where Γ is the interaction parameter. A convenient reference and lower bound to the total potential energy is the Madelung energy of a bcc lattice,[2]

$$\beta E_{\text{static}} = -1.791\,86\Gamma . \tag{2}$$

For very low densities ($\Gamma < 1$) the system is represented by the Debye-Huckel model and it has been shown that this model predicts exactly the long-range correlations for any Γ. Let $S(k)$ be the usual structure factor. Then Stillinger and Lovett[4] (SL) have shown that for small values of k the structure factor will go to the Debye-Huckel value,

$$S(k) = k^2/3\Gamma . \tag{3}$$

Fourier inversion of this equation gives two important moment conditions on the two-particle correlation function $g(r)$,[4]

$$\rho \int d^3r\,[g(r) - 1] = -1 , \tag{4}$$

$$\rho \int d^3r\, r^2 [g(r) - 1] = -2/\Gamma . \tag{5}$$

For larger values of Γ, direct simulation of the system is the only accurate way of computing properties of the OCP. Brush, Sahlin, and Teller's[1] original Monte Carlo calculations with the Ewald image potential have recently been refined and extended to higher densities by Hansen.[2] Pollack and Hansen[5] have estimated the liquid-solid phase transition to be at the density $\Gamma = 155 \pm 10$, by doing careful computations in the liquid and solid phases of the energy, and using the usual double-tangent construction.

Perturbation methods

A number of different perturbation methods have been proposed in the literature to calculate the properties of a system with long-range forces in terms of one with short-range forces.[6-9] We have chosen to use a method based on the two-particle correlation function since this contains the important properties of the equilibrium bulk system and is readily comparable to other work. Let $v_0(r)$ be the reference potential and $g_0(r)$ its exact correlation function. Suppose a long-range Coulomb tail $\Delta v(r)$ is added to the reference potential, so that the sum of the reference potential and the Coulomb tail is equal to the original full Coulomb potential, $v(r) = v_0(r) + \Delta v(r)$. If a cluster expansion in the range of the potentials is made, the change to lowest order in the correlation function is[6]

$$g(r) = g_0(r) + H(r) , \tag{6}$$

where

$$H(r) = -\frac{1}{\rho(2\pi)^3} \int d^3k\, e^{i\vec{k}\cdot\vec{r}} \frac{\Delta v(k) S_0^2(k)}{1 + \Delta v(k) S_0(k)} , \tag{7}$$

and $S_0(k)$ is the reference-system structure function,

$$S_0(k) = 1 + \rho \int d^3r\, e^{i\vec{k}\cdot\vec{r}} [g_0(r) - 1] , \tag{8}$$

and $\Delta v(k)$ is the Fourier transform of the change of potential,

$$\Delta v(k) = \rho \int d^3r\, e^{i\vec{k}\cdot\vec{r}} [v(r) - v_0(r)] . \tag{9}$$

From Eqs. (7)–(9) the perturbed structure function is simply

$$S(k) = 1/[\Delta v(k) + 1/S_0(k)] . \tag{10}$$

If the reference system is sufficiently short range (see Appendix B for the conditions) then the structure function S_0 will be positive[10] for all k. But since $\Delta V(r)$ consists of a long-range Coulomb potential tail then for small k, $\Delta v(k) = 3\Gamma/k^2$. Then from Eq. (10), it is clear that the perturbed $S(k)$ will have the Stillinger-Lovett form [Eq. (3)] for sufficiently small k. However $g(r)$ in Eq. (6) is not necessarily positive for small r; this formula is really only good for large r and this serious defect must be remedied.

An alternative calculation yields[4] for the perturbed correlation function

$$g(r) = g_0(r) e^{+H(r)} . \tag{11}$$

This will give the same result as before for large r, and $g(r)$ will be positive for all r, but the SL conditions will not be satisfied.

A reformulation of the perturbation procedure by Lado[8] allows us to have both of these desirable properties. The following identity may be obtained by analyzing the graphs obtained in a cluster expansion of $g(r)$:

$$g(r) = \exp[B(r) - v(r) + g(r) - c(r) - 1] , \tag{12}$$

where $c(r)$ is the direct correlation function and $B(r)$ is the bridge function. (Consult Ref. 11 for a discussion of the definitions of these functions and the relationships between them.) The normal HNC (hypernetted chain) equation is obtained from Eq. (12) by setting $B(r) = 0$. In Lado's method the bridge function is evaluated in the reference system; it is assumed that a long-range perturbation will not change it in an important way; then Eq. (12) is used to calculate the correlation function in the per-

turbed system. We shall call this method the reference-HNC method (RHNC). This method is the same as solving the pure HNC equation for a potential $v(r) - B_0(r)$, where $B_0(r)$ is the bridge function in the reference system. The bridge function is a way of correcting for the inaccuracy of the pure-HNC equation. The numerical method we used to carry out this perturbation scheme is that suggested by Lado,[8] and is described in Appendix A.

It is not known for which potentials the pure-HNC equation will have solutions; numerical solutions have been found for many physical potentials.[12] If a physical solution exists to Eq. (12), both $g(r)$ and $S(k)$ will be non-negative. The solution of this equation[13] will satisfy the SL conditions and thus give the correct behavior for small k—see Appendix B. The following sections discuss our choice of the reference system potential, the evaluation by Monte Carlo of the reference-system correlation functions $g_0(r)$ and $S_0(k)$, and the extension of $g_0(r)$ to infinity.

Short-range system

The perturbation method requires that we evaluate the two-particle correlation function in a short-range system. For the method to be accurate the short-range potential must be similar to the Coulomb potential. The potentials should clearly have the same behavior for small r (except for a constant shift in energy), but since we want to use the "cutoff convention"[3] in the simulation, the potential must vanish for interparticle separations greater than $\frac{1}{2}$ the simulation box edge. Another criterion that has been suggested[9] is that the Fourier transform of the change of potential $\Delta v(k)$ should go quickly to zero for large k. From the definition of $H(r)$ [Eq. (7)], if $\Delta V(k)S_0(k) \leq -1$, $H(k)$ will have a singularity, and it is unlikely any perturbative series would converge. A sufficient condition to ensure that $H(k)$ remains finite is $\Delta V(k) \geq 0$. This criterion precludes merely truncating the Coulomb potential at the box edge for the range of Γ being considered.

The reference potential that we have used in the Coulomb potential times a complementary error function is denoted

$$v_0(r) = \Gamma \operatorname{erfc}(r/\sigma)/r\,, \tag{13}$$

where σ is an adjustable range parameter. This potential is like a Coulomb potential for $r/\sigma \ll 1$, but for large r it goes to zero very quickly,

$$v_0(r) \sim (\Gamma\sigma/\sqrt{\pi})e^{-(r/\sigma)^2}/r^2, \quad r \gg \sigma\,. \tag{14}$$

To satisfy the cutoff convention σ must be chosen so that $v_0(L/2) \ll 1$. This potential converges much more quickly than a Yukawa potential for large r. In addition, v_0 possesses a positive, quickly convergent Fourier transform,

$$v_0(k) = (4\pi\Gamma/k^2)\rho(1 - e^{-(k\sigma)^2/2})\,. \tag{15}$$

Finally, it is the same as the lowest-order (with the usual convergence function) spherically symmetric part[1] of the Ewald image potential with $\sigma = L\sqrt{\pi}$. We expect the short-range correlations of the two potentials to be the same, since they are so similar for small r.

Monte Carlo simulation

With this choice of reference potential we have evaluated $g_0(r)$ and $S_0(k)$ using the standard, well tested, Metropolis algorithm[14] for simulating a classical fluid, where

$$g_0(\vec{r}_1, \vec{r}_2) = \frac{N(N-1)\int d\vec{r}_3 \cdots \int d\vec{r}_N \exp[-\sum_{i<j} v_0(r_{ij})]}{\rho^2 \int d\vec{r}_1 \cdots \int d\vec{r}_N \exp[-\sum_{i<j} v_0(r_{ij})]} \tag{16}$$

and

$$S_0(\vec{k}) = \left\langle \frac{1}{N} \left| \sum_{i=1}^{N} e^{i\vec{k}\cdot\vec{r}_i} \right|^2 \right\rangle, \quad \vec{k} = \frac{2\pi}{L}\vec{n} \tag{17}$$

and N is the number of particles and $\rho = N/L^3$. Brush *et al.*[1] describe the Monte Carlo algorithm methods for testing the convergence of the Markov chain, and a method of recording $g_0(r)$. Usually the number of particles in the box was 128, with occasional calculations with more particles; each particle was moved about 10^3 times, and periodic boundary conditions were used. The results for the reference system are shown in Table I. The quantities E_0, P_0, and S_0 are the classical potential energy, the excess pressure (i.e., not including the thermal pressure) and the value of $S_0(k)$ at $k = 0$, respectively.

Figure 3 shows $g_0(r)$ for three different values of σ at $\Gamma = 75$. The results have been smoothed and extended by the technique described in the following section. In the next section we show, with a χ^2 test, that the smoothed $g_0(r)$ is statistically consistent with the original data. Figure 1 shows $g_0(r)$ for $\Gamma = 120$ and $\sigma = 1.5$ with 128 and 256 particles. The curves are again due to the extension technique. While the differences for the two different particle numbers are not large, they are significant and are probably the major source of error in this calculation. This difference is an example of a bias in $g_0(r)$ because the Monte Carlo simulation is of a finite system.

EXTENDING THE TWO-PARTICLE CORRELATION FUNCTION

For input into our perturbation equations we need the two-particle correlation function and the struc-

TABLE I. Results for the reference potential and perturbation-method RHNC with interaction parameters Γ and σ [see Eq. (13)]; N is the number of particles in the Monte Carlo simulation, N_m is the number of moves per particle in the Markov chain; E_0, P_0, and S_0 are, respectively, the classical potential energy per particle, the excess pressure per particle, and the structure factor at $k=0$ in the reference system; g_{max} is the maximum value of $g(r)$ for the OCP with the RHNC equation; ΔE is the energy per particle relative to the Madelung energy as calculated by the RHNC equation. The entries marked ∞(H) or ∞(BST) are from Refs. 1 and 2.

Γ	σ	N	N_m ($\times 10^{-3}$)	E_0	P_0	S_0	g_{max}	ΔE [a]
50	1.5	128	1	17.853	28.06	0.015	1.67	1.73
	∞(BST)						1.655	1.70 ± 0.02
75	0.8	128	1	1.34	3.55	0.059	1.70	2.28
	1.0	128	1	4.21	9.57	0.040	1.74	2.17
	1.5	128	2	26.17	41.85	0.010	1.87	1.97
	∞(BST)						1.920	1.94 ± 0.03
100	1.2	128	0.5	13.27	26.21	0.016	2.00	2.19
	∞(H)						2.06	2.12 ± 0.04
120	1.1	128	1	10.11	21.98	0.018	2.07	2.40
	1.5	128	1	40.86	66.29	0.004	2.26	2.18
	1.5	256	0.3	41.01		0.006	2.17	2.25
	∞(H)						2.19	2.23 ± 0.07
140	1.4	128	1	36.10	62.36	0.007		2.36
	∞(H)						2.32	2.34 ± 0.1

[a] The errors quoted in this column we obtained from comments made in Hansen's papers (Ref. 2).

ture function in the reference system. The equations are quite sensitive to these functions, and if one is to have reliable results, $g_0(r)$ and $S_0(k)$ must both be made smooth, continuous, non-negative functions, and mutually consistent. The Monte Carlo simulation only finds $g_0(r)$ for r less than half the box length but the correlations will extend much further than that. In addition, there is both

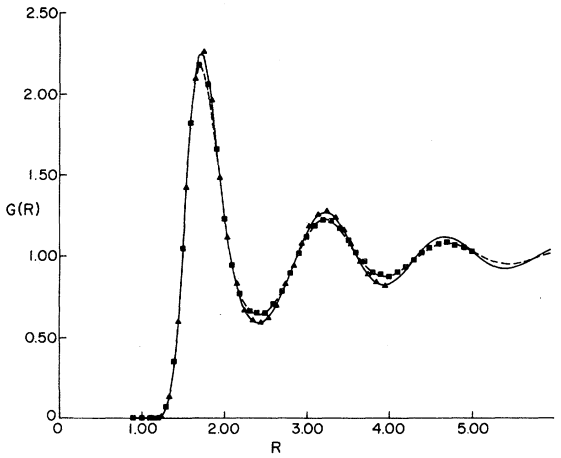

FIG. 1. $g_0(r)$ versus r (in reduced units) for the error-function potential at $\Gamma=120$ and $\sigma=1.5$. The squares are the MC data for 256 particles, the triangles for 128 particles. Through each set of data is fitted a curve of the form of Eq. (19) with $J=3$. The smaller system seems to have more structure.

a random error in the estimates of g_0 and S_0 (because the Markov chain has a finite length) and a systematic bias (because the Monte Carlo box is finite). Before we present the method we have used for doing this extension and smoothing, we will discuss three other methods.

The simplest method[15] is to assume some form for $g_0(r)$ outside the box. Let $g_E(r_i)$ and $S_E(k_i)$ be the actual Monte Carlo estimates of $g_0(r)$ and $S_0(k)$. Now assume a trial value for g_0,

$$g_0(r) = \begin{cases} g_E(r_i), & r \lesssim L/2 \\ 1, & r > L/2 . \end{cases} \tag{18}$$

Then Fourier transform this assumed form [Eq. (8)] to get S_0. Typically this function will become negative for small k and not agree with S_E. Correct the S_0 in the small-k region by some method to agree with S_E and again transform to get g_0. Correct the g_0 in the interior region to get agreement with g_E and continue iterating until consistency is reached. The g_0 resulting from this procedure will be smooth and consistent with the Monte Carlo estimates; however, this procedure is clearly not unique (M independent values of S_E can determine at most the value of g_0 at M different values of r in the exterior region) and, in particular, will not necessarily give the correct asymptotic form to $g_0(r)$. For the OCP one could require that the extended $g(r)$ satisfy the two SL moment conditions. However, we are only inter-

ested in extending the radial distribution function for the short-range system and the values of its moments are not known.

A method that has worked well for hard-core liquids[16] is to assume that for r greater than some extension point r_E the Percus-Yevick equation is satisfied, and for $r<r_E$, $g_0(r)$ equals the Monte Carlo estimate $g_E(r)$. This is enough to determine a unique g_0 in the exterior region.[17] However, when this procedure was tried with the soft-core fluid, a sizable discontinuity appeared at the extension point r_E in g_0, regardless of where the extension point was. The same discontinuity appears when the HNC equation is used instead of the PY equation. The problem is that neither of these equations is very good even for large r, for this fluid. The bridge function (Fig. 6) is nonzero for r inside the box and it cannot be neglected.

Usually the Monte Carlo system is chosen to be a cube with periodic boundary conditions. We have experimented with boxes that are much longer in one direction, with the intent of increasing the range of $g_E(r)$. However, it appears that the $g_0(\vec{r})$ for this narrow box has much more directional dependence than the $g_0(r)$ for a cube. In particular, the average number of long-wavelength density fluctuations [i.e., $S_0(k)$] in the short dimensions was much less than in a cube, while the number in the long direction was more for the same wave-vector. The correlation function $g_0(r)$, for large r, was of course primarily averaged across the long direction and contained this bias. Also, for a finite system, g_0 does not tend toward unity for large separations, but toward $1-1/N$, and this effect could be seen for a long narrow box. A long thin box is not as good a representation of bulk matter as is a cubic box with the same number of particles. In summary, we have found that each of the extension methods we have just described leads to a $g_0(r)$ different from that of infinite bulk matter in some significant way.

The way we have chosen to extend the two-particle correlation function is to assume that for r greater than the position of the first peak, $g_0(r)$ will be equal to a sum of damped oscillations and find those parameters which best fit the Monte Carlo data. For r in the interval $r_F<r<L/2$, where r_F is the value of r at the maximum of $g_0(r)$, $g_0(r)$ is assumed to be of the form

$$g_0(r)=1+\sum_{j=1}^{J}\frac{1}{r}\,\mathrm{Re}\{A_j e^{z_j r}\}\,, \tag{19}$$

where A_j and z_j are complex parameters and $J=1,2,3$. This form was suggested by Kirkwood[18] on the basis of a simple argument with a hard-sphere fluid. An asymptotic form like Eq. (19) has been shown to be consistent with the correlation function of a classical Lennard-Jones liquid.[16] It has also been shown that the solution of both the HNC and PY equations for large r behave this way.[19] This type of $g(r)$ results from the structure function having simple poles at $k=\pm iz_j$ and being analytic as a function of k^2 at the origin.[12]

To check the assumption about the form of $g(r)$ we have performed a statistical χ^2 test. For a given value of r_F and J, χ^2 is minimized with respect to the parameters A_j and z_j, where

$$\chi^2=\sum_{i=r_F}^{L/2}\frac{[g_E(r_i)-g_0(r_i)]^2}{V_{g_i}} +\sum_{i=1}^{k_n}\frac{[S_E(k_i)-S_0(k_i)]^2}{V_{k_i}}\,, \tag{20}$$

and V_{g_i} and V_{k_i} are the variances of the Monte Carlo estimate of $g(r_i)$ and $S(k_i)$. [Only the k values inside the first peak of $S(k)$ are included in the sum as the others are not statistically significant.] If the fit is valid χ^2 should be equal to the number of degrees of freedom (number of independent r_i and k_i points minus $4J$). There is, of course, some correlation between the quantities in the sum. The variance of the estimate of $g(r_i)$ has been calculated for this algorithm:

$$V_{g_i}=Cg_0(r_i)/N_m\rho\,dV_i\,. \tag{21}$$

N_m is the number of moves used to estimate $g(r_i)$, dV_i is the volume of the interval, and C is a constant (independent of r) and dependent on details of the algorithm (such as the acceptance ratio) but usually between 2 and 3.

The results of the χ^2 fit verify our assumption about the behavior of $g(r)$. The χ^2 test is quite severe since where there were often as many as 100 degrees of freedom, the accuracy for many of the points was as small as 0.5% and $g_0(r)$ was followed through $1\frac{1}{2}$ oscillations. The inclusion of the terms in $S(k)$ in Eq. (20) requires that the asymptotic behavior of the $g_0(r)$ be correct. The results of our fit indicate that the series in Eq. (19) is quickly convergent for values of r greater than one interparticle spacing. For smaller distances this form is clearly inappropriate. We find that for $\Gamma<100$ two terms are sufficient for a good fit, otherwise three terms are enough. The wave vector of the main oscillation is chiefly determined by the density. We find that roughly

$$I_m(z_1)=4.25(4\pi\rho/3)^{1/3} \tag{22}$$

for all values of σ and Γ. The other wave numbers are roughly multiples of this value.

Shown in Fig. 1 are the Monte Carlo results (g_E) for 128- and 256-particle systems, in triangles

and squares, respectively. The smoothed and extended results are shown as solid curves. The wave number and phase seem to agree in the extended region; the difference in amplitude is a system size effect. With this extension we have calculated the two-particle correlation function for the OCP using Eq. (12). As we have already pointed out, this is easily done because Eq. (12) with $B(r)$ replaced with $B_0(r)$ is equivalent to the HNC equation with a potential $V(r)$-$B_0(r)$.

RESULTS AND DISCUSSION

The energies and the maximum value of $g(r)$ obtained from the perturbation-method RHNC are shown in Table I for several values of Γ and σ. The energy is quite constant with respect to the irrelevant parameter σ and is very close to the energies computed with the Ewald image method.[1,2] There is some inaccuracy when either the number of particles in the Monte Carlo reference system, or the value of σ, is too small. However, it is computationally feasible to choose a system large enough and a σ large enough so that one can compute the energy as accurately as with the Ewald image method. (See Fig. 2, and Table I).

The two-particle correlation functions calculated from RHNC are also very close to those computed by the image method. Figures 3 and 4 show $g(r)$'s at $\Gamma=75$ and $\Gamma=120$ with several values of σ. The triangles are from the image method. The best perturbation results, those with the largest values of σ and most particles, are indistinguishable from the Ewald $g(r)$'s, except for a small difference at the peak of this function. If the Ewald image method is inaccurate one would expect some dependence on the size of the system. The published values[2] of $g_{max}(r)$ show it to be quite constant as a function of the number of particles. Hence the small differences in $g(r)$ between the Ewald image method and the RHNC method are probably due to inaccuracies in our calculation.

The use of the Ewald image method is most dubious at moderately high densities, the range of

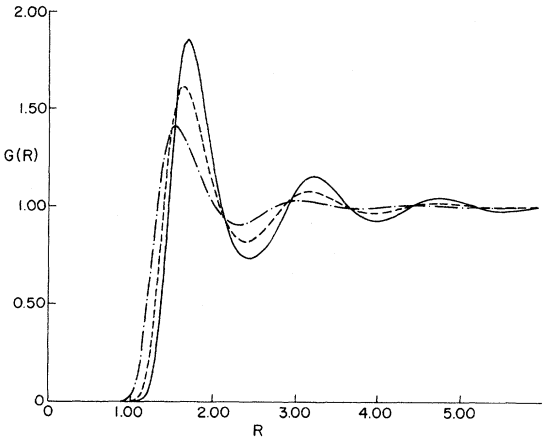

FIG. 3. $g_0(r)$ versus r for the error-function potential at $\Gamma=75$ and three values of σ (0.8, 1.0, and 1.5); the higher values of σ correspond to a greater maximum value at the peak $g_0(r)$. All three curves have been smoothed and extended by the method described in the text.

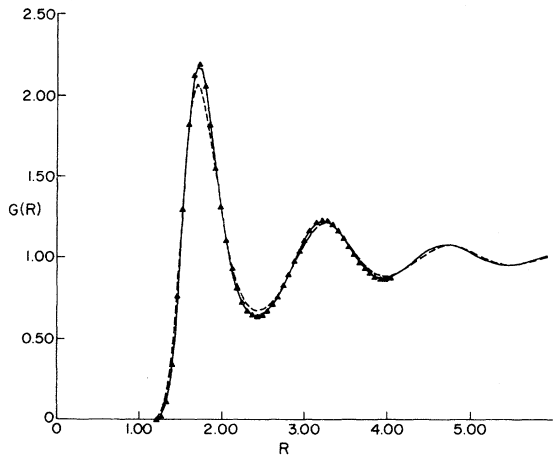

FIG. 2. $g(r)$ versus r for the OCP at $\Gamma=120$. The triangles are MC data from the Ewald image method (Hansen, Ref. 2). The two curves are the results of the perturbation-method RHNC. The solid curve is evaluated from a reference system with 256 particles and $\sigma=1.5$. The dashed curve is with 128 particles and $\sigma=1.1$.

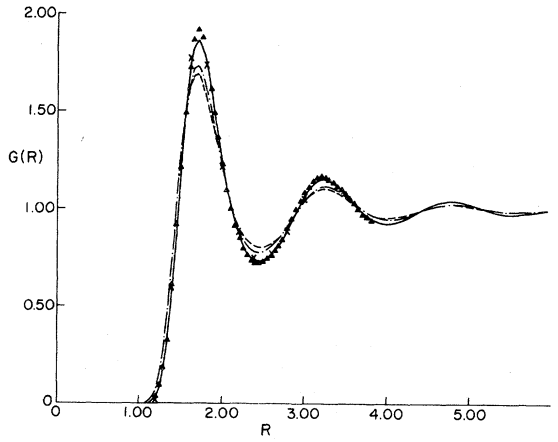

FIG. 4. $g(r)$ versus r for the OCP at $\Gamma=75$. The triangles are from Ref. 1 and the Ewald image method. The $\times$'s are from Ref. 12 and are the result of using the bridge function of Eq. (23). The three curves are the result of using the RHNC method on the $g_0(r)$ in Fig. 3. The reference system had $\Gamma=75$ and $\sigma=0.8$, 1.0, 1.5. The higher values of σ correspond to higher magnitudes at the maximum of $g(r)$.

Γ covered in this paper—at low densities any computational method should do well; in the solid phase the Ewald technique should work very well. However, in the one-component plasma, the polarization of the simulation cube is zero if the center of mass is fixed (only one type of charges is free to move). For this reason the OCP may not be a good system to test the validity of the Ewald method. In systems with two components free to move, Valleau and Whittington's argument[3] concerning polarization correlations may be relevant. Our treatment (RHNC) is not subject to the same objections as is the Ewald method. The simulation takes place among short-range particles and putting in the Coulomb potential is done for an infinite system in an electrostatically valid manner. We believe that this result establishes the validity of both the RHNC method and the Ewald image method applied to the OCP.

The results of the simpler perturbation formula given in Eq. (11) are shown in Table II, for $\Gamma = 75$ and three values of σ. Figure 5 shows the corresponding $g(r)$'s. The energies and the first and second moments of $g(r)$ are in all cases much less accurate than those given by RHNC. The results do seem to be converging to the correct values but it is clear that the perturbing potential must be quite small for this method to work.

The bridge function $B_0(r, \Gamma, \sigma)$ for $\Gamma = 75$ and several values of σ is shown in Fig. 6. Since $B_0(r)$ is negative, the effective HNC potential $v_0 - B_0$ is more repulsive than the reference potential v_0. The bridge function is an order of magnitude smaller than the reference potential, but appears to have roughly the same range. It must be noted that the calculation of this function is quite sensitive to fluctuations in, and the extension of, the Monte Carlo data.

A recent paper[12] has solved the HNC equation assuming the following form for the OCP bridge function:

TABLE II. Results for the OCP at $\Gamma = 75$ using perturbation equation (11). σ is the potential cutoff parameter in Eq. (13); ΔE is the potential energy relative to the Madelung energy; S_0 is the value of the structure factor at $k = 0$; $S_0^{(2)}$ is the coefficient proportional to K^2 [see Eq. (3)]. All quantities are dimensionless. The entry ∞(H) is from Ref. 2.

σ	ΔE	S_0	$S_0^{(2)}$ ($\times 10^3$)
0.8	11.576	+0.092	−83.83
1.0	2.659	−0.102	−11.52
1.5	2.452	+0.011	−1.83
∞(H)	1.94 ± 0.03	0.0	−4.44

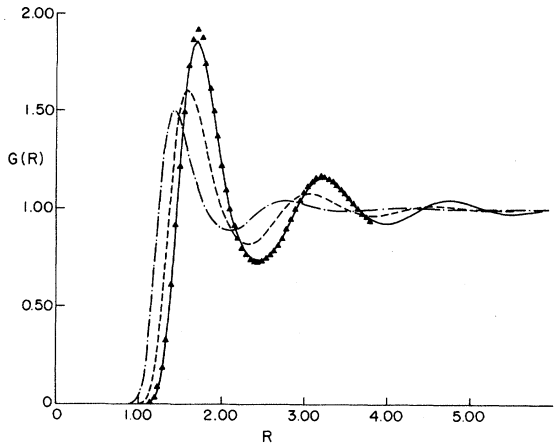

FIG. 5. $g(r)$ versus r for the OCP at $\Gamma = 75$. The triangles are again from Ref. 1 and the Ewald image method. The three curves are the result of using the lowest-order perturbation equation (8) (applied to the g_0's shown in Fig. 3). The reference system had $\Gamma = 75$ and $\sigma = 0.8$, 1.0, 1.5. The higher values of σ correspond to higher magnitudes at the maximum of $g(r)$. Comparison of this with Fig. 4 shows that the approximate equation doesn't do nearly so well for the lower two values of σ.

$$B_N(r) = -0.6\,\mathrm{erf}(0.024\Gamma)\Gamma/r\,. \tag{23}$$

On Fig. 4 the resulting $g(r)$ is marked with ×'s. It seems to have the correct behavior. But because $B_N(r)$ goes as r^{-1} at large r the resulting structure function will have the wrong behavior for small k,

$$S_N(k) = k^2/3\Gamma[1 + 0.6\,\mathrm{erf}(0.024\Gamma)]\,. \tag{24}$$

In order for the SL conditions to be satisfied the

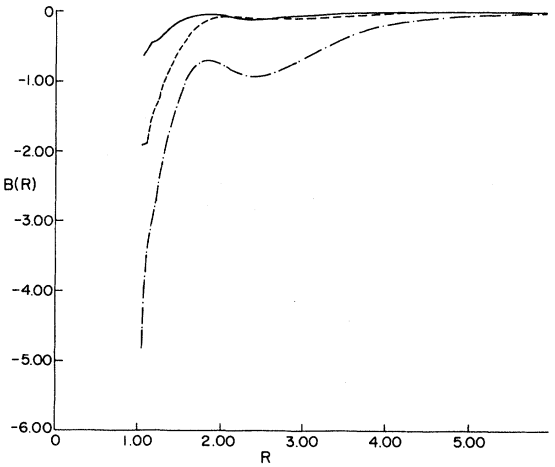

FIG. 6. Bridge function $B(r, \Gamma, \sigma)$ versus r for $\Gamma = 75$ and three values of σ (0.8, 1.0, 1.5). The higher values of σ correspond to larger magnitudes of B. The $g_0(r)$ are shown in Fig. 3. This function is assumed to be constant with respect to σ in the RHNC method.

correct $B(r)$ for the OCP must go to zero at large r faster than r^{-1}. See Appendix B for the proof. The agreement between the $g(r)$'s suggests strongly that $g(r)$ is not too sensitive to the large-r behavior of the effective HNC potential.

A surprising feature of the RHNC method is that $B_0(r, \Gamma, \sigma)$ depends somewhat sensitively on σ, yet the perturbed $g(r)$, and also the reference $g_0(r)$, converges to the OCP $g(r)$. The reason for this convergence is that the short-range potential gives us just the right short-range correlations in $g(r)$ and all the perturbation equation needs to do is handle the long-range correlations due to the Coulomb potential—which it does exactly. If one regards the SL conditions as specifying the zero and second moments [see Eqs. (4) and (5)] of the OCP $g(r)$, the potential energy is proportional to the -1 moment. So with a $g(r)$ at all reasonable, it is likely the energy will be fairly accurate. This argument helps to explain why the energies predicted by the pure-HNC equation are fairly accurate[20] for large Γ.[12,21]

APPENDIX A: NUMERICAL METHOD OF SOLVING THE PERTURBATION EQUATIONS

To use the RHNC perturbation method a pair of coupled nonlinear equations for the two-particle correlation function $g(r)$ and the direct correlation function $c(r)$ must be solved. The mathematical problem is the same as the problem of solving the pure-HNC equation with an effective potential of $v(r) - B_0(r)$. A function without a subscript describes the perturbed system (g) and a zero subscript indicates the reference system (g_0).

In the reference or short-range system the two-particle correlation function $g_0(r)$, its Fourier transform, the structure function $S_0(k)$ [Eq. (8)], and the direct correlation function $c_0(k)$,

$$c_0(k) = 1 - 1/S_0(k), \tag{A1}$$

are known. The bridge function $B_0(r)$ is defined in the reference system by Eq. (12) with $v(r) = v_0(r)$. We assume $B(r)$ is the same for the Coulomb system.

Following a procedure very similar to that suggested by Lado[4] we make the following change of variables. Eliminate the functions g, S, B, v, and c and write the perturbation equations in terms of the following functions:

$$\begin{aligned} H(r) &= \ln[g(r)/g_0(r)], \\ \Delta c(r) &= c(r) - c_0(r), \\ \Delta v(r) &= v(r) - v_0(r). \end{aligned} \tag{A2}$$

Subtract the logarithm of the HNC equation (12) in the reference system from that in the perturbed system. The bridge function drops out and using definitions (A2) we get the following equation:

$$\Delta c(r) = g_0(r)(e^{H(r)} - 1) - H(r) - \Delta v(r). \tag{A3}$$

The other coupled equation can be found by noting that the difference in the two-particle correlation function is simply

$$\begin{aligned} \Delta g(r) &= g_0(e^{H(r)} - 1) \\ &= \frac{1}{(2\pi)^3 \rho} \int d^3k \, e^{i\vec{k}\cdot\vec{r}} [S(k) - S_0(k)]. \end{aligned} \tag{A4}$$

Apply the relation (A3) between $S(k)$ and $c(k)$ and rewrite this equation in terms of S_0 and Δc:

$$g_0(r)(e^{H(r)} - 1) = \frac{1}{(2\pi)^3 \rho} \int d^3k \, e^{i\vec{k}\cdot\vec{r}} \left(\frac{S_0^2 \Delta c(k)}{1 - S_0 \Delta c(k)} \right). \tag{A5}$$

The advantage of this form of the equations is that $H(r)$ will be constant for small r, not change over many orders of magnitude, while $B_0(r)$ will not even be defined for small r because there $g_0(r)$ (from Monte Carlo) is identically zero. In doing the Fourier transform to get $\Delta c(k)$, the term involving $\Delta v(r)$ should be done analytically, otherwise with the Coulomb potential the result will depend on the upper limit of the integral.

We solve the perturbation equation iteratively. Initially assume $H(r)$ is zero and with Eq. (A3) find $\Delta c(r)$. Define

$$\begin{aligned} F(r) = \frac{1}{(2\pi)^3 \rho} \int d^3k \, e^{i\vec{k}\cdot\vec{r}} \left[\frac{S_0^2(k) \Delta c(k)}{1 - S_0(k) \Delta c(k)} \right] \\ - g_0(r)(e^{H(r)} - 1). \end{aligned} \tag{A6}$$

Use Eq. (A6) to find $F(r)$. If $F(r)$ were zero then both equations (A3) and (A5) would be satisfied. Note that if we let

$$H_{n+1}(r) = H_n(r) + F_n(r), \tag{A7}$$

the result for $g(r)$ after one iteration will be the same as Eq. (11). If one uses Eq. (A7) and iterates, after a few interactions the process is unstable; the successive $H(r)$'s become increasingly large. The usual method of preventing this instability by mixing the old and new H's also works here:

$$H_{n+1}(r) = H_n(r) + \alpha F_n(r). \tag{A8}$$

For stability α must be quite small at these densities ($\alpha < 0.1$).

The criteria that we chose for convergence was that $|F_n(r)| < 10^{-5}$ and the zeroth and second moments [Eqs. (4) and (5)] should be accurate to a relative error of 10^{-5}. The above mixing method took several hundred to one thousand iterations to reach this accuracy.

One can speed up the convergence by an order of magnitude by assuming the operator $F(H(r))$ is linear in the region near the solution H_∞. Then if our current function H_n is close to the solution H_∞ and we have iterated long enough so that only those eigenvectors with large eigenvalues remain, one can write

$$F(H_n)=\lambda(H_n-H_\infty). \tag{A9}$$

Suppose at iteration n we have saved the results of two previous iterations,

$$\begin{aligned} H_{n-1}&=H_{n-2}+\alpha F(H_{n-2}),\\ H_n&=H_{n-1}+\alpha F(H_{n-1}). \end{aligned} \tag{A10}$$

Then if Eq. (A9) is valid the following ratio should be constant:

$$\gamma(r)=F(H_{n-1})/F(H_{n-2}). \tag{A11}$$

If the function does indeed turn out to be constant we do not use equation (A8) to find the next H but we try to subtract out the remaining eigenvector,

$$H_n=H_{n-1}+F(H_{n-1})/\lambda, \tag{A12}$$

where the eigenvalue λ is estimated from

$$\lambda=\langle[\gamma(r)-1]/\alpha\rangle. \tag{A13}$$

This scheme makes the convergence very quick in the latter stages.

Fast Fourier transforms were used to speed up iterations of the equations. It was found that the use of any integration formula other than the trapezoidal rule amplified the noise in $g_0(r)$ and $S_0(k)$ and the solutions were less accurate. The grid in both r and k must be quite small for accurate solutions. In dimensionless units one must have $dx<0.01$ for the zeroth moment of $g(r)$ to be accurate and $dk<0.06$ for the second moment of $g(r)$ and for the energy to be accurate.

APPENDIX B: PROPERTIES OF SOLUTIONS OF THE RHNC METHOD

The perturbation method used in this paper (RHNC) is based on the generalized HNC equation [Eq. (12)]:

$$g(r)=\exp[g(r)-c(r)-1-v(r)-B(r)], \tag{B1}$$

where $c(r)$ is the direct correlation function defined in terms of $g(r)$ [Eq. (A1)] and $V-B$ acts as a rescaled HNC potential. Although numerical solutions to the HNC equation have been found for a variety of potentials, the conditions for a unique physical solution are not known. We will assume that for any rescaled HNC potential, one can always find a solution to Eq. (B1) satisfying the following physical conditions: both $g(r)$ and the corresponding $S(k)$ should both be finite and continuous everywhere and go to unity for large r and k, respectively. Clearly Eq. (B1) also implies that $g(r)$ is nonnegative everywhere. If $c(k)$ is to be finite everywhere (except at $k=0$) then from Eq. (A1), $S(k)$ must be positive everywhere except at $k=0$. If $c(r)$ is to be finite and if

$$\lim_{k\to 0} S(k)=ak^m \tag{B2}$$

we must require that $m<3$.

In this appendix we will show that a solution to the perturbation-method RHNC will have the correct behavior for small r and for the OCP it will obey the SL conditions [Eqs. (3)–(5)]. Let us make the following assumptions about the reference-system potential $v_0(r)$ and the Coulomb potential $v_c(r)$:

(i) v_0 is short range, infinitely repulsive at the origin, and a lower bound exists for the potential energy,

$$\lim_{r\to\infty} r^3 v_0(r)=0, \tag{B3}$$

$$\lim_{r\to 0} v_0(r)=+\infty, \tag{B4}$$

$$\sum_{i<j} v_0(r_{ij})>BN \tag{B5}$$

for any set of coordinates $\{r_i\}$, $i=1,\ldots,N$.

(ii) v_c is Coulombic,

$$\lim_{r\to\infty} r^3[v_c(r)-\Gamma/r]=0 \tag{B6}$$

for some Γ.

(iii) v_0 and v_c have a similar core,

$$\lim_{r\to 0} r^3[v_c(r)-v_0(r)]=0. \tag{B7}$$

First let us show that under assumptions (B3)–(B5) the reference-system bridge function is finite everywhere. It can be shown[22] that $g_0(r)$ must go like $e^{-v_0(r)}$ for small r:

$$0\le\lim_{r\to 0}[\ln g_0(r)+v_0(r)]<+\infty. \tag{B8}$$

Also for a short-range repulsive potential isothermal compressibility is positive[10]:

$$\chi\propto\lim_{k\to 0} S_0(k)=1+\rho\int d^3r\,[g_0(r)-1]>0. \tag{B9}$$

But by definition

$$C_0(r)=\frac{1}{(2\pi)^3\rho}\int d^3k\, e^{i\vec{k}\cdot\vec{r}}\left(1-\frac{1}{S_0(k)}\right). \tag{B10}$$

Then $C_0(r)$ must be finite everywhere since the integrand is finite everywhere and $S_0(k)$ goes to unity at large r.

Rewrite Eq. (B1) as

$$B(r)=\ln g_0+v_0+C_0(r)+1-g_0(r). \tag{B11}$$

All of the terms on the right-hand side are finite everywhere; hence $B(r)$ is.

Now we wish to show that for small r the perturbed $g(r)$ will behave like $e^{-v_c(r)}$. But this is clear from the equivalent of Eq. (B11) in the Coulomb system,

$$\ln g + v_c = B(r) - c(r) - 1 + g(r). \tag{B12}$$

Since we have just shown that $B(r)$ is finite for all r, and we can show the same to be true for $c(r)$, it follows from this equation that $g(r)$ has the correct behavior.

Now let us show that the small-k behavior of $S(k)$ is that given by the Stillinger-Lovett conditions. Eliminate $\Delta c(r)$ from the perturbation equations (A3) and (A5) for $S(k)$. After some manipulation we get the relation

$$S(k)^2 - S(k)[\Delta v(k) + S_0(k) + 1/S_0(k) + H(k)] + 1 = 0, \tag{B13}$$

where $H(r)$ and $\Delta v(r)$ are defined in Eq. (A2). Compare this relation to the simpler equation (10). For $k=0$, $H(k)$ is finite since for large r, $H(r)$ goes to zero like $g(r) - g_0(r)$ and for small r, $H(r)$ behaves like $\Delta v(r) + \text{const}$, and from condition (B7), v_0 and $v(r)$ have the same core. The other term, $S_0(k) + 1/S_0(r)$, also remains finite at small k [Eq. (B9)]. Hence the low-k behavior of $S(k)$ is determined by $\Delta v(k)$, and by condition (B6) its small-k behavior is

$$\Delta v_0(k) = 3\Gamma/k^2; \tag{B14}$$

then for small k, $S(k)$ will go to the Debye-Huckel value [Eq. (3)].

A solution of the pure-HNC equation will also obey the SL conditions since the pure-HNC equation is recovered by choosing the reference system to be an ideal gas. This low-k behavior for a solution of the HNC equation in the case of the one-component plasma has been noted before in the literature.[12,19] Suppose one constructs a family of short-range potentials $v_0(r, \sigma)$ which converge to the Coulomb potential,

$$\lim_{\sigma\to\infty} v_0(r, \sigma) = v_c(r). \tag{B15}$$

Then one would expect the perturbation method (RHNC) to be arbitrarily good for large σ. With this assumption the above result is a rederivation of the Stillinger-Lovett result.

Finally, it is clear that the bridge function $B(r, \Gamma)$ *for the OCP* must go to zero faster than $1/r$ at large r. Otherwise the $1/r$ coefficient of the rescaled HNC potential $v(r) - B(r)$ would not be equal to Γ and the second moment of $g(r)$ would not be given by Eq. (5).

---

*Supported by the Energy Research and Development Administration under Contract No. E(11-1)-3077 and by Grant DMR-74-23494 with the National Science Foundation, and in part by the National Science Foundation through the Materials Science Center, Cornell University, under Grant DMR-72-03029, Technical Report No. 2657.

[1]S. G. Brush, H. L. Sahlin, and E. Teller, J. Chem. Phys. 45, 2102 (1966).

[2]J. P. Hansen, Phys. Rev. A 8, 3096 (1973).

[3]J. P. Valleau and S. G. Whittington (unpublished).

[4]F. H. Stillinger and R. Lovett, J. Chem. Phys. 49, 1991 (1968).

[5]E. L. Pollack and J. P. Hansen, Phys. Rev. A 8, 3110 (1973).

[6]J. L. Lebowitz, G. Stell, and S. Baer, J. Math. Phys. 6, 1282 (1965); P. C. Hemmer, J. Math. Phys. 5, 75 (1964).

[7]F. Lado, Phys. Rev. A 8, 2548 (1973).

[8]F. Lado, Phys. Rev. 135, A1013 (1964).

[9]H. C. Andersen and D. Chandler, J. Chem. Phys. 55, 1497 (1971).

[10]J. Ginibre, Phys. Lett. 24A, 223 (1967).

[11]S. A. Rice and P. Gray, *Statistical Mechanics of Simple Liquids* (Wiley, New York, 1965); see particularly pp. 95–100.

[12]Kin-Chue Ng., J. Chem. Phys. 61, 2680 (1974); P. Hutchinson and W. R. Conkie, Mol. Phys. 3, 567 (1972).

[13]It is worth noting that solutions of the unmodified HNC equation also satisfy the SL conditions.

[14]N. A. Metropolis, A. W. Rosenbluth, A. H. Teller, and E. Teller, J. Chem. Phys. 21, 1087 (1953).

[15]M. H. Kalos, D. Levesque, and L. Verlet, Phys. Rev. A 9, 2178 (1974).

[16]L. Verlet, Phys. Rev. 165, 201 (1968).

[17]Verlet asserts (Ref. 16) that there is no discontinuity in $g_0(r)$ at r_E if $g_E(r_E) = 1$. We believe this is incorrect. If the PY equation is nearly satisfied in the exterior region, as it is for hard-core fluids, the discontinuity will be small.

[18]J. G. Kirkwood, J. Chem. Phys. 7, 919 (1939).

[19]A. A. Broyles, S. U. Chung, and H. L. Sahlin, J. Chem. Phys. 37, 2462 (1962).

[20]The HNC equation overestimates the excess energy by 10% at $\Gamma=20$ and 26% at $\Gamma=140$. This error is computed from the formula $(E_{\text{HNC}} - E_{\text{Ewald}})/(E_{\text{Ewald}} - E_{\text{static}})$. The HNC energies are from Refs. 13 and 14, the Ewald energies from Ref. 2.

[21]J. F. Springer, M. A. Pokrant, and F. A. Stevens, J. Chem. Phys. 58, 4863 (1973).

[22]B. Widom, J. Chem. Phys. 39, 2808 (1963).